EFFICIENT SAMPLING ON HEALPIX GRID

Adeem Aslam† , *Zubair Khalid*† , *Member, IEEE, and Rodney A. Kennedy*⋆, *Fellow, IEEE*

† School of Science and Engineering, Lahore University of Management Sciences, Lahore, Pakistan
⋆ Research School of Engineering, The Australian National University, Canberra, ACT 2601, Australia
Email: adeem.aslam@uet.edu.pk, zubair.khalid@lums.edu.pk, rodney.kennedy@anu.edu.au

ABSTRACT

We propose an iso-latitude sampling scheme for the representation of band-limited signals on the sphere. The proposed scheme is designed as a variant of the widely used Hierarchical Equal Area iso-Latitude Pixelization (HEALPix) on the sphere. We use HEALPix grid of resolution $N_{\rm side}$ to represent a signal of band-limit (spherical harmonic degree) L. To reduce the number of samples, the proposed algorithm takes only L iso-latitude rings out of $4N_{\rm side} - 1$ rings of the HEALPix. This selection is carried out by ensuring that the spherical harmonic transform (SHT) of the signal can be computed accurately from the samples. The number of samples required by the proposed sampling scheme is smaller than those required by HEALPix by at least a factor of $3/2$. For the proposed sampling scheme, we also formulate the spherical harmonic transform and conduct numerical experiments to evaluate the number of samples required by the proposed sampling scheme and the accuracy of associated SHT.

Index Terms— Sampling, HEALPix, unit 2-sphere, spherical harmonic transform, band-limited signals

1. INTRODUCTION

There are many disciplines of science and engineering in which signals exhibit angular dependence and hence, are inherently defined on the sphere. Areas where spherical signal processing techniques have been extensively used include wireless communication [1], computer graphics [2], medical imaging [3], acoustics [4], quantum chemistry [5], cosmology [6] and geodesy [7], to name a few. In many of these applications, signal is often analysed in the spatial or harmonic domain. The transformation from the spatial to harmonic domain is enabled by spherical harmonic transform (SHT).

As we can only process spatially discrete signals, many sampling schemes have been proposed for the computation of SHT [8–12]. Equiangular sampling schemes (e.g. [9, 10]) enable exact computation of SHT but suffer from massive over-sampling near the poles which renders them sub-optimal and even useless for certain applications. Equal area and iso-latitude tessellation schemes are most desirable because not only do they avoid over-sampling at the poles, they enable separation of variables which supports faster computation of SHT. One of the widely adopted such scheme is the Hierarchical Equal Area iso-Latitude Pixelization (HEALPix) [12]. It supports hierarchical structure for storing samples which is realized as an essential requirement for dense sampling grids, facilitating various topological methods of analysis and allowing for fast computation of transforms through fast look-up of neighboring data samples. SHT associated with the HEALPix utilizes all the samples on the grid to evaluate the transform as an approximate quadrature. Although, HEALPix supports accurate computation of SHT, it is a high-resolution sampling grid and therefore, it is very desirable to design a sampling scheme that maintains the same order of accuracy in the computation of SHT but takes fewer number of samples.

Rodney A. Kennedy is supported by the Australian Research Council's Discovery Projects funding scheme (Project no. DP170101897).

In this context, we address the following research questions in this work:

1. Can we reduce the number of samples required by the HEALPix sampling grid for the computation of SHT?
2. Does the proposed reduction in the number of samples compromise the accuracy of the SHT?

In addressing these questions, we organize the rest of the paper as follows. In Section 2, we review the mathematical background for signal and harmonic analysis on the sphere and present an overview of the HEALPix sampling scheme. In Section 3, we formulate the SHT, outline the sampling requirements and present an algorithm to design the sampling scheme. Before we present the concluding remarks in Section 5, we evaluate the reduction in number of samples achieved by the proposed sampling scheme and carry out the accuracy analysis of the formulated transform in Section 4.

2. MATHEMATICAL PRELIMINARIES

In this section, we present the necessary mathematical background for spatial and spectral representation of signals on the sphere and review the HEALPix sampling scheme.

2.1. Signals on 2-Sphere

We consider complex-valued functions $f(\theta, \phi)$ on the 2-sphere (or sphere), denoted by $\mathbb{S}^2$. Here $\theta \in [0, \pi]$ is the co-latitude angle measured from the positive z-axis and $\phi \in [0, 2\pi]$ is the longitude angle measured from the positive x-axis in the x-y plane. The inner product between two such functions f, g is given by

$$\langle f, g\rangle \triangleq \int_{\mathbb{S}^2} f(\theta,\phi)\overline{g(\theta,\phi)} \sin\theta d\theta d\phi, \tag{1}$$

where $\overline{(\cdot)}$ denotes the complex conjugate operation, $\sin\theta d\theta d\phi$ is the differential area element on the sphere and integration is carried out over the whole sphere, i.e., $\int_{\mathbb{S}^2} = \int_{\theta=0}^{\pi}\int_{\phi=0}^{2\pi}$. With the inner product defined in (1), the set of functions on the sphere form a Hilbert space $L^2(\mathbb{S}^2)$. Energy and norm of the signal f are given by $\langle f, f\rangle$ and $\|f\| \triangleq \langle f, f\rangle^{1/2}$ respectively.

2.2. Spherical Harmonics

The Hilbert space $L^2(\mathbb{S}^2)$ is separable and contains a complete set of orthonormal basis functions referred to as spherical harmonic functions or spherical harmonics for short, defined as [13]

$$Y_\ell^m(\theta,\phi) \triangleq \sqrt{\frac{2\ell+1}{4\pi}\frac{(\ell-m)!}{(\ell+m)!}}P_\ell^m(\cos\theta)e^{im\phi}, \qquad (2)$$

for integer degree $\ell \geq 0$ and order[1] $|m| \leq \ell$. Here $P_\ell^m(\cos\theta)$ is the associated Legendre polynomial of degree ℓ and order m [13]. Since spherical harmonics form a complete set of orthonormal basis functions on the sphere, any signal $f \in L^2(\mathbb{S}^2)$ can be expressed as

$$f(\theta,\phi) = \sum_{\ell=0}^{\infty}\sum_{m=-\ell}^{\ell}(f)_\ell^m Y_\ell^m(\theta,\phi), \qquad (3)$$

where

$$(f)_\ell^m = \langle f, Y_\ell^m\rangle = \int_{\mathbb{S}^2} f(\theta,\phi)\overline{Y_\ell^m(\theta,\phi)}\sin(\theta)d\theta d\phi \qquad (4)$$

is the spherical harmonic (spectral) coefficient of degree ℓ and order m and constitutes the spectral representation of the signal. The transformation (spatial to spectral) of the signal in (4) is referred to as the spherical harmonic transform (SHT) and the one (spectral to spatial) given in (3), is referred to as the inverse SHT (ISHT). A signal is considered band-limited at degree L if $(f)_\ell^m = 0$ for $\ell, m \geq L$. Set of all such band-limited signals on the sphere forms an L^2-dimensional subspace of $L^2(\mathbb{S}^2)$ and is denoted by $\mathcal{H}_L$. For any signal $f \in \mathcal{H}_L$, the sum over degree in (3) is truncated at $L-1$.

2.3. Hierarchical Equal Area iso-Latitude Pixelization (HEALPix)

Hierarchical equal area iso-Latitude pixelization [12], HEALPix for short, takes three iso-latitude rings of samples with four samples in each ring, dividing the sphere into 12 equal area regions at the base-resolution level. Sampling grid density is parameterized by $N_{\rm side}$ which is defined as the number of divisions along the side of a base-resolution pixel needed to reach a desired high-resolution tessellation. An increase in resolution level by one divides each of the equal area regions on the sphere into four sub-regions. Total number of samples on HEALPix sampling grid are $12N_{\rm side}^2$ and are placed into three zones: Equatorial ($-2/3 < z < 2/3$), North polar ($z \leq -2/3$) and South polar ($z \geq 2/3$), where $z = \cos(\theta)$. Total number of iso-latitude rings on the sampling grid is $4N_{\rm side} - 1$ out of which $2N_{\rm side} - 1$ are located in the equatorial zone and $N_{\rm side}$ are located in each polar zone. All equatorial rings contain maximum number of samples per ring, equal to $4N_{\rm side}$, whereas the polar zone rings contain varying number of samples.

SHT associated with the HEALPix is computed by the approximate quadrature rule[2] given by

$$\widehat{(f)}_\ell^m = \frac{4\pi}{N_{\rm pix}}\sum_{k=0}^{N_{pix}-1} f(\theta_k,\phi_k)\overline{Y_\ell^m(\theta_k,\phi_k)}. \qquad (5)$$

Since the quadrature approximation in (5) is the zeroth-order estimator, the Jacobi iterative method is applied on it to improve its accuracy.

[1] $|\cdot|$ denotes the absolute value

[2] http://healpix.sourceforge.net/documentation.php

3. EFFICIENT SPHERICAL HARMONIC TRANSFORM FOR HEALPIX

Now we address the first question posed in Section 1 and propose an algorithm for the computation of spherical harmonic transform of the band-limited signal $f \in \mathcal{H}_L$ using only a subset of samples on the HEALPix grid. We propose to take samples on L iso-latitude rings with locations indexed in the vector $\theta \equiv [\theta_0, \theta_1, \ldots, \theta_{L-1}]^T$. Before we determine the location of these iso-latitude rings and the number of samples along each ring, we present the formulation of SHT.

3.1. Spherical Harmonic Transform – Formulation

For a signal $f \in \mathcal{H}_L$, its spherical harmonic coefficients of order $|m| < L$ can be defined in terms of the Fourier transform of the signal along ϕ in an iso-latitude ring placed at $\theta = \theta_k$ as

$$\begin{aligned} G_m(\theta_k) &\triangleq \int_0^{2\pi} f(\theta_k,\phi)e^{-im\phi}d\phi \\ &= 2\pi\sum_{\ell=|m|}^{L-1}(f)_\ell^m \tilde{P}_\ell^m(\theta_k), \end{aligned} \qquad (6)$$

where $\tilde{P}_\ell^m(\theta_k) \triangleq Y_\ell^m(\theta_k, 0)$ is the scaled associated Legendre polynomial. By defining a column vector $\mathbf{g}_m$ as a vector of Fourier transform of the signal at $L-|m|$ different iso-latitude rings, given by

$$\mathbf{g}_m \triangleq \left[G_m(\theta_{|m|}), G_m(\theta_{|m|+1}), \ldots, G_m(\theta_{L-1})\right], \qquad (7)$$

and a column vector $\mathbf{f}_m$ containing spherical harmonic coefficients of order m as

$$\mathbf{f}_m \equiv \left[f_{|m|}^m, f_{|m|+1}^m, \ldots, f_{|L-1|}^m\right], \qquad (8)$$

we can compactly express $L-|m|$ equations of the form given in (6) as

$$\mathbf{g}_m = 2\pi\mathbf{P}_m\mathbf{f}_m, \quad |m| < L, \qquad (9)$$

where

$$\mathbf{P}_m \triangleq \begin{bmatrix} \tilde{P}_{|m|}^m(\theta_{|m|}) & \tilde{P}_{|m|+1}^m(\theta_{|m|}) & \cdots & \tilde{P}_{L-1}^m(\theta_{|m|}) \\ \tilde{P}_{|m|}^m(\theta_{|m|+1}) & \tilde{P}_{|m|+1}^m(\theta_{|m|+1}) & \cdots & \tilde{P}_{L-1}^m(\theta_{|m|+1}) \\ \vdots & \vdots & \ddots & \vdots \\ \tilde{P}_{|m|}^m(\theta_{L-1}) & \tilde{P}_{|m|+1}^m(\theta_{L-1}) & \cdots & \tilde{P}_{L-1}^m(\theta_{L-1}) \end{bmatrix}. \qquad (10)$$

It becomes clear from (10) that in order for $\mathbf{P}_m$ to be well-conditioned, Fourier transform in (6) must be evaluated on at least L different iso-latitude rings. By computing $G_m(\theta_k)$ at different iso-latitude rings placed at $\theta_k, k = |m|, |m|+1, \ldots, L-1$ and inverting $\mathbf{P}_m$ in (9), we can compute the spherical harmonic coefficients of order m and degrees $|m| \leq \ell \leq L-1$.

3.2. Spherical Harmonic Transform – Computation

The spherical harmonic coefficients of order m contained in vector $\mathbf{f}_m$ can be recovered from (9) provided $\mathbf{g}_m$ is computed correctly and $\mathbf{P}_m$ is well-conditioned to be invertible. Consequently, the accuracy of the proposed transform is dictated by the computation of $G_m(\theta_k)$ and inversion of $\mathbf{P}_m$. Accurate computation of

$G_m(\theta_k)$ depends on the number of samples along ϕ in the chosen iso-latitude ring and the condition number of $\mathbf{P}_m$ depends on the locations $\theta_{|m|}, \theta_{|m|+1}, \ldots, \theta_{L-1}$ of the iso-latitude rings.

3.2.1. Avoiding Aliasing in the Computation of $G_m(\theta_k)$

Using (6) and changing the order of summation in (3), a signal f band-limited at L and evaluated at samples in an arbitrary iso-latitude ring placed at θ_k can be written as

$$f(\theta_k, \phi) = \frac{1}{2\pi} \sum_{m=-(L-1)}^{L-1} G_m(\theta_k) e^{im\phi} \tag{11}$$

We observe that this signal has contribution from $2L-1$ complex exponentials $e^{im\phi}, |m| \leq L$. We therefore, require at least $2L-1$ samples in the ring placed at θ_k to avoid the effects of aliasing on $G_m(\theta_k)$. This is true regardless of the choice of the ring. However, we note that if we know spherical harmonic coefficients of order $|m| \leq p \leq L-1$, we can subtract the contribution of these spherical harmonic coefficients from the samples of the signal in the iso-latitude ring placed at $\theta_{|m|-1}$, if this ring does not have $2L-1$ samples. This ring is then required to have only at least $2|m|-1$ samples for $G_{|m|-1}(\theta_{|m|-1})$ to be free of any aliasing errors. We further elaborate on this concept. Equation (9) can be used to solve for $(f)_{L-1}^{L-1}$ by computing $G_{L-1}(\theta_{L-1})$ on a ring placed at θ_{L-1} and having at least $2L-1$ samples. If the next ring at θ_{L-2} has at least $2L-1$ samples, we compute $G_{L-2}(\theta_{L-2})$ without aliasing. However, if the number of samples is less than $2L-1$ but at least $2L-3$, then we have to subtract the contribution of $(f)_{L-1}^{L-1}$ and $(f)_{L-1}^{-(L-1)}$ from the samples of f in the ring placed at θ_{L-2} and update it as

$$f(\theta_{L-2}, \phi) \leftarrow f(\theta_{L-2}, \phi) - \tilde{f}_{L-1}(\theta_{L-2}, \phi), \tag{12}$$

where

$$\begin{aligned}\tilde{f}_m(\theta_k, \phi) &= \sum_{\ell=|m|}^{L-1} \{(f)_\ell^m \tilde{P}_\ell^m(\theta_k) e^{im\phi} + (f)_\ell^{-m} \tilde{P}_\ell^{-m}(\theta_k) e^{-im\phi}\} \\ &= \frac{1}{2\pi}(G_m(\theta_k) e^{im\phi} + G_{-m}(\theta_k) e^{-im\phi})\end{aligned} \tag{13}$$

is the contribution of spherical harmonic coefficients of order m and $-m$ for all degrees $|m| \leq \ell \leq L-1$. Hence, we require the iso-latitude ring at θ_{L-1} to have at least $2L-1$ samples, the iso-latitude ring at θ_{L-2} to have at least $2L-3$ samples and so on.

3.3. Sampling Scheme – Requirements

Following the philosophy presented in the previous section and using the formulation given in (9), we note that the SHT of the signal band-limited at L can be accurately computed by taking samples of the signal over iso-latitude sampling scheme of L rings located at $\theta_k,\ k = 0, 1, \ldots, L-1$, provided the sampling scheme fulfills the following requirements:

(R1) The iso-latitude ring located at θ_k has *at least* $2k+1$ samples along longitude.

(R2) Ring locations, $\theta_k,\ k = 0, 1, \ldots, L-1$ are chosen such that the matrix $\mathbf{P}_m$ given in (10) is well-conditioned for each[3] $m = 0, 1, \ldots, L-1$.

[3]We only need to ensure that $\mathbf{P}_m$ is well-conditioned for non-negative orders m as $\mathbf{P}_{-m} = (-1)^m \mathbf{P}_m$ which follows from the conjugate symmetry of spherical harmonics given by $Y_\ell^{-m}(\theta, \phi) = (-1)^m \overline{Y_\ell^m(\theta, \phi)}$.

SHT can be computed accurately if sampling scheme design takes into account these requirements as R1 and R2 ensure the accurate computation of $\mathbf{g}_m$ and accurate inversion of (10) for each $|m| < L$ respectively.

3.4. Sampling Scheme – Design

We devise an algorithm to design the sampling scheme comprised of subset of HEALPix samples. Before we present the algorithm that selects the iso-latitude rings of samples from HEALPix taking into account the sampling requirements, we establish a relationship between the HEALPix parameter N_{side} and band-limit L. Since the number of samples required in the first ring is $2L-1$ and all the rings in equatorial zone on the HEALPix grid contain maximum number of samples per ring, i.e., $4N_{\text{side}}$, the first ring must be chosen from the equatorial zone. This puts an upper bound on the band-limit of the signal, that is, $L \leq 2N_{\text{side}}$. Hence, for a given sampling grid with resolution parameter N_{side}, we can compute the SHT for a maximum band-limit of $2N_{\text{side}}$.

To select the iso-latitude rings of samples from HEALPix grid with resolution parameter N_{side}, we propose the following iso-latitude ring selection algorithm taking into account R1 and R2. We use $\tilde{\theta}_h$ and n_h to denote the location of iso-latitude ring and the number of samples along ϕ in it with $h = 1, 2, \ldots, H$, where $H = 4N_{\text{side}} - 1$ is the total number of rings on the HEALPix grid.

Procedure 1 Ring Selection Algorithm

Require: $\theta_k,\ k = 0, 1, \ldots, L-1$
procedure RING SELECTION($\tilde{\theta}_h$, N_{side})
    $\Theta = \{\tilde{\theta}_h\}_{h=1}^{H}$
    $\theta_{L-1} = \pi/2$ (first ring)
    for $m = L-2, L-3, \ldots, 0$ **do**
        $\Theta_m = \{\tilde{\theta}_h \in \Theta \mid n_h \geq 2m+1\}$
        Choose $\theta_m \in \Theta_m$ which minimizes the condition number of $\mathbf{P}_m$
    end for
    return $\theta_k,\ k = 0, 1, \ldots, L-1$.
end procedure

The proposed algorithm identifies the rings from the HEALPix grid in such a way that each $\mathbf{P}_m$ matrix is well-conditioned and at the same time has at least $2k+1$ samples along ϕ in the ring located at θ_k, thus serving both sampling design requirements and ensuring the accurate computation of SHT.

3.5. Multipass SHT

Like HEALPix, we also employ an iterative method to further improve the transform. After computing the spectral coefficients in the first pass, we reconstruct the signal in spatial domain using (3). Spectral coefficients of the difference between original and reconstructed spatial signals are computed and added to the previously computed coefficients, obtaining the spectral coefficients in the second pass. This process is continued until the error between original and reconstructed spatial signals converges.

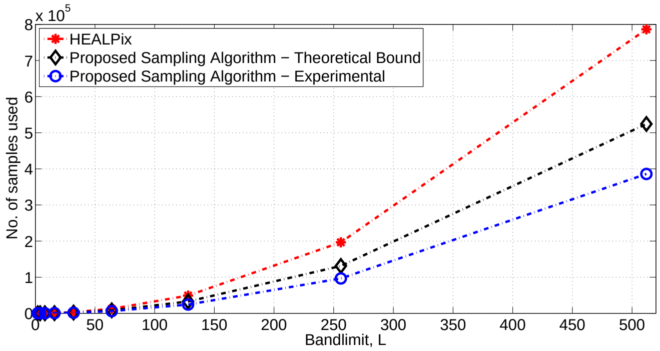

Fig. 1: Number of samples used by HEALPix and proposed sampling scheme along with the theoretical bound established in Lemma 1 for band-limits in the range $2 \leq L \leq 512$.

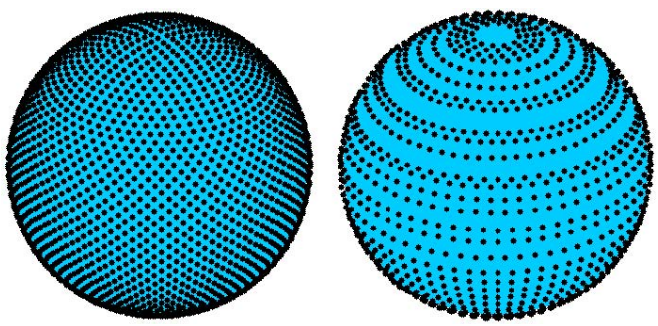

Fig. 2: Visual comparison of sampling density between HEALPix and proposed sampling scheme for bandlimit, $L = 32$.

4. EVALUATION

In this section, we compare the accuracy of the formulated SHT with SHT associated with the HEALPix and evaluate the reduction in number of samples achieved by the proposed sampling scheme. The formulated SHT is efficient compared to the one associated with the HEALPix in the sense that it uses lesser number of samples to accurately compute the spectral coefficients.

4.1. Reduction in Number of Samples

Since the proposed ring selection algorithm chooses the iso-latitude rings on the HEALPix grid by minimizing the condition number of the matrix $\mathbf{P}_m$, we cannot analytically determine the exact decrease in the number of samples achieved by the proposed sampling scheme. However, we can work out the minimum guaranteed decrease in the number of samples which is presented in the following Lemma.

Lemma 1 (Lower-bound on the Reduction in Number of Samples)**.** *The proposed sampling scheme requires at least $3/2$ times less number of samples than HEALPix for the accurate computation of SHT of the signal band-limited at $L \leq 2N_{\rm side}$.*

Proof. Since $L_{\max} = 2N_{\rm side}$ denotes the maximum band-limit for a given grid resolution parameter $N_{\rm side}$ and the number of samples on the HEALPix grid is $N_{\rm pix} = 12N_{\rm side}^2$, we have $L_{\max} = \sqrt{N_{\rm pix}/3}$. As the proposed sampling scheme requires $L(\leq L_{\max})$ iso-latitude rings for the accurate computation of SHT, the number of samples in the proposed sampling scheme, denoted by N, is given by $N \leq L(4N_{\rm side}) \leq L_{\max}(4N_{\rm side})$ or $N_{\rm pix}/N \geq 3/2$. □

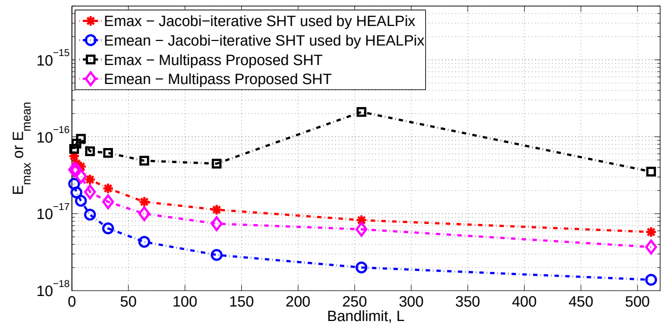

Fig. 3: $E_{\rm max}$ and $E_{\rm mean}$ between spectral coefficients of the original and reconstructed signals for band-limits in the range $2 \leq L \leq 512$.

In Fig. 1, we plot the number of samples used by SHT associated with the HEALPix, number of samples required by SHT formulated for the proposed sampling scheme and the theoretical bound established in Lemma 1 for band-limits in the range $2 \leq L \leq 512$. It can be seen that at moderately large band-limits, the proposed sampling scheme, in comparison with HEALPix, requires about half the number of samples. Fig. 2 provides a visual comparison of the number of samples used by HEALPix and proposed sampling scheme to compute SHT accurately for bandlimit, $L = 32$.

4.2. Accuracy Analysis

SHT formulated for the proposed sampling scheme is evaluated on the test signal generated using test spectral coefficients, $(f_T)_\ell^m$, uniformly distributed between -1 and 1 in real and imaginary parts. We denote by $(f_R)_\ell^m$ the reconstructed spectral coefficients. For both the sampling schemes, we evaluate the maximum and mean errors defined as

$$E_{\rm max} \triangleq \frac{1}{\|f_T\|} \max |(f_T)_\ell^m - (f_R)_\ell^m|, \qquad (14)$$

$$E_{\rm mean} \triangleq \frac{1}{\|f_T\|} \sum_{\ell=0}^{L-1} \sum_{m=-\ell}^{\ell} |(f_T)_\ell^m - (f_R)_\ell^m|. \qquad (15)$$

These errors are averaged over ten different realizations of the test signal for band-limits in the range $2 \leq L \leq 512$ and plotted in Fig. 3. It is evident that the proposed sampling scheme, although requires less number of samples, enables accurate computation of SHT with errors on the order of numerical precision.

5. CONCLUSIONS

We have presented an iso-latitude sampling scheme on the sphere as a variant of the widely used Hierarchical Equal Area iso-Latitude Pixelization (HEALPix) sampling scheme for the representation and reconstruction of band-limited signals on the sphere. The proposed sampling scheme requires at least $3/2$ times less number of samples than HEALPix to accurately compute spherical harmonic transform (SHT) of the signal. We have also conducted numerical experiments, demonstrating the accurate computation of SHT with errors on the order of numerical precision.

6. REFERENCES

[1] T. S. Pollock, T. D. Abhayapala, and R. A. Kennedy, "Introducing space into MIMO capacity calculations," *J. Telecommun. Syst.*, vol. 24, no. 2, pp. 415–436, Oct. 2003.

[2] R. Ng, R. Ramamoorthi, and P. Hanrahan, "Triple product wavelet integrals for all-frequency relighting," *ACM Trans. Graph.*, vol. 23, no. 3, pp. 477–487, Aug. 2004.

[3] M. K. Chung, K. M. Dalton, L. Shen, A. C. Evans, and R. J. Davidson, "Weighted fourier series representation and its application to quantifying the amount of gray matter," *IEEE Trans. Med. Imag.*, vol. 26, no. 4, pp. 566–581, Apr. 2007.

[4] W. Zhang, M. Zhang, R. A. Kennedy, and T. D. Abhayapala, "On high-resolution head-related transfer function measurements: An efficient sampling scheme," *IEEE Trans. Acoust., Speech, Signal Process.*, vol. 20, no. 2, pp. 575–584, 2012.

[5] D. W. Ritchie and G. J. L. Kemp, "Fast computation, rotation, and comparison of low resolution spherical harmonic molecular surfaces," *Journal of Computational Chemistry*, vol. 20, no. 4, pp. 383–395, 1999.

[6] D. N. Spergel, R. Bean, O. Doré, M. R. Nolta, C. L. Bennett, J. Dunkley, G. Hinshaw, N. Jarosik, E. Komatsu, L. Page, H. V. Peiris, L. Verde, M. Halpern, R. S. Hill, A. Kogut, M. Limon, S. S. Meyer, N. Odegard, G. S. Tucker, J. L. Weiland, E. Wollack, and E. L. Wright, "Three-year Wilkinson Microwave Anisotropy Probe (WMAP) observations: Implications for cosmology," *The Astrophysical Journal Supplement Series*, vol. 170, no. 2, pp. 377–408, 2007.

[7] M. A. Wieczorek and F. J. Simons, "Minimum variance multitaper spectral estimation on the sphere," *J. Fourier Anal. Appl.*, vol. 13, no. 6, pp. 665–692, 2007.

[8] Z. Khalid, R. A. Kennedy, and J. D. McEwen, "An optimal-dimensionality sampling scheme on the sphere with fast spherical harmonic transforms," *IEEE Trans. Signal Process.*, vol. 62, no. 17, pp. 4591–4610, Sep. 2014.

[9] J. R. Driscoll and D. M. Healy, Jr., "Computing Fourier transforms and convolutions on the 2-sphere," *Adv. Appl. Math.*, vol. 15, no. 2, pp. 202–250, Jun. 1994.

[10] J. D. McEwen and Y. Wiaux, "A novel sampling theorem on the sphere," *IEEE Trans. Signal Process.*, vol. 59, no. 12, pp. 5876–5887, Dec. 2011.

[11] R. G. Crittenden and N. G. Turok, "Exactly azimuthal pixelizations of the sky," *Arxiv preprint astro-ph/9806374*, 1998.

[12] K. M. Górski, E. Hivon, A. J. Banday, B. D. Wandelt, F. K. Hansen, M. Reinecke, and M. Bartelmann, "HEALPix: A Framework for High-Resolution Discretization and Fast Analysis of Data Distributed on the Sphere," *Astrophys. J.*, vol. 622, pp. 759–771, Apr. 2005.

[13] R. A. Kennedy and P. Sadeghi, *Hilbert Space Methods in Signal Processing*. Cambridge, UK: Cambridge University Press, Mar. 2013.